ITER reflectometry diagnostics operation limitations

caused by strong back and small angle scattering

E.Z. Gusakov[1], S. Heuraux[2], A.Yu. Popov[1]

[1] *Ioffe Institute, St.Petersburg, Russia*

[2] *IJL, UMR-CNRS 7198, Vandoeuvre CEDEX, France*

1. Introduction

The microwave reflectometry is considered nowadays as key diagnostics in ITER, for plasma positioning, density profile reconstruction, and also able to provide measurements on turbulence. Both O-mode and X-mode reflectometers launching probing wave from high and low magnetic field side are developed [1]. On ITER, the fast frequency sweep reflectometer [1] should be able to diagnose very flat density profiles, which correspond to long probing wave paths (several meters). Under these unfavorable conditions the reflectometers can suffer from destructive influence of plasma turbulence which may lead on one hand to multiple small angle scattering or strong phase modulation and on the other hand to a strong Bragg backscattering (BBS) or to an anomalous reflection. In the first case the probing beam looses coherence and therefore the standard approaches to characterize the turbulence are no more applicable, whereas in the second – the wave reflection occurs far from the cut-off position thus complicating the density profile reconstruction.

In this paper the turbulence level thresholds for strong phase modulation and strong BBS are derived for different probing modes and frequencies. Relativistic corrections to the plasma permittivity due to the high electron temperature were included, which induces a spatial shift of the O-mode and X-mode cut-off positions [3]. Results obtained for two scenarios (one with a rather flat density profile, $n_0 = 1.2\cdot 10^{20} m^{-3}$, $n_{edge} = 0.8\cdot 10^{20} m^{-3}$, $B_0 = 5\ T$ and the other with the absolutely flat density profile shown in [2], $n_0 = n_{edge} = 1\cdot 10^{20} m^{-3}$, $B_0 = 5\ T$) are discussed in detail. For both cases with the considered reflectometers, it is shown that the scattering transition into the non-linear regime occurs at the level of turbulent density perturbation comparable or below that found in the present day tokamak experiments. The threshold of strong phase modulation is given by $\delta n / n_0 \sim 0.05 \div 0.5\%$, whereas the threshold of strong BBS is estimated as $\delta n / n_0 \sim 0.5 \div 3\%$ depending on the mode used and the frequency. A new approach to turbulence diagnostics based on radial correlation reflectometry useful in the case of strong phase modulation is introduced. The possibility of local monitoring of turbulence behavior in this case is discussed.

2. Physical model and analytical approach to the non linear BBS regime

Considering an incident ordinary or extraordinary wave propagating perpendicular to the external magnetic field, we treat it assuming slab plasma geometry in the framework of the Helmholtz equation

$$E_\alpha'' + k_\alpha^2(x)E_\alpha + \delta k_\alpha^2(x)E_\alpha = 0, \quad (1)$$

where $\alpha = o$ and $\alpha = e$ correspond to the ordinary mode and extraordinary mode, respectively, $E_o \equiv E_z$, $E_e \equiv E_y$, k_α and δk_α are unperturbed wave vector and perturbation of the wave vector due to the perturbation of the background density $\overline{n}(x)$ given by $\delta n(x) = \delta n_0 \exp\left[-(x - x_{BR})^2 / L^2\right]\cos(\kappa x)$, where $\kappa L >> 1$. It is modeling a quasi-coherent turbulent fluctuation localized in a position of the corresponding Bragg resonance (BR) where the BBS condition $\kappa = 2k(x_{BR})$ is fulfilled. We solve (1) numerically and investigate its solutions analytically using methods developed in the three wave interaction theory. In the later case assuming weak plasma inhomogeneity we seek a solution to (1) in the form of the incident and reflected WKB waves propagating in both directions with the amplitudes a_i and a_r being constant everywhere except possibly the vicinity of the BR points, where due to BBS they vary slowly. The scale of this variation given by $l = \left|dk_\alpha / dx\right|_{x_{BR}}^{-1/2}$ is intermediate, much longer than the probing wave-length and much smaller than the refractive index gradient scale length, allowing us to obtain the following reduced differential equations for amplitudes:

$$il\frac{d}{dx}a_i + \sqrt{Z}a_r \exp(i\Phi) = 0, il\frac{d}{dx}a_r - \sqrt{Z}a_i \exp(-i\Phi) = 0, \quad (2)$$

where $Z = (\omega/c)^4\left[h_\alpha \cdot \delta n_0 / n_c \cdot l/\kappa\right]^2$ is a slowly varying function, $\Phi(x) = \int_{x_{BR}}^{x}\left[2k_\alpha(x') - \kappa\right]dx'$ is a phase mismatch caused by plasma inhomogeneity and an explicit expression for the numerical coefficient h_α could be found in [4]. The system (2) was analyzed in detail in the theory of three-wave parametric decay instability. In the case of non-localized perturbation ($L \to \infty$) its solutions are expressed in terms of the parabolic cylinder functions describing coupling of the incident and reflected waves in the vicinity of the BR in detail. However, for practical applications this too detailed information is not needed.

3. Limitations of fluctuation reflectometry caused by strong BBS.

Characteristics of BBS provided by solution of (2) most important practically are transmission and reflection coefficients

$$S_{ii,rr} = \exp\left(-\frac{\pi Z}{2}\right), \; S_{ri,ir} = \mp\exp\left(\pm i\frac{\pi}{4}\right)2\sqrt{\frac{\pi}{Z}}\frac{\exp(-\pi Z/4)}{\Gamma(\mp iZ/2)} \quad (3)$$

for the waves incident onto the BR layer from the edge and from the cut-off, respectively. They relate the asymptotic expressions for the electric field on both sides of the BR. Then we assume the only fluctuation in plasma and no cut off as shown in figure 1 by black dashed line. We can see that in spite of the fact the density perturbation is much smaller than the background density in the BR, so that no cut-off is produced, the strong suppression of the wave transmission through the BR layer is observed in figure 1. The interpretation of this strong effect may be given in terms of strong BBS using expression (3) directly. Moreover, using (2) the expression for the incident wave amplitude can be obtained in the form $\exp\left(-\int_{x_1}^{x}\sqrt{|Z(\xi)|-\xi^2}\,d\xi\right)$ with x_1 being smaller of the roots of a transcendental equation $|Z(\xi)|-\xi^2=0$ perfectly describing the reduction of the electric field in the BR layer (see black solid curve in figure 1). The comparison of the transmission coefficient dependence on the relative density perturbation given by (3) and computed numerically has resulted in reasonable agreement, as it is seen in figure 2. An important feature of the transmission coefficient is its exponential dependence on the parameter Z and thus on the fluctuation amplitude squared. In the case of $Z>>1$ ($S_{ii}\big|_{Z>>1}\to 0$, $S_{ir,ri}\big|_{Z>>1}\approx\exp(\mp i\varphi)$, where $\varphi=\varphi(Z)$) this dependence leads to suppression of transmission and to 100% reflection of the incident wave due to BBS. In this limit a picture of the wave propagation resembles total reflection of the incident wave from the BR region with an additional phase φ imposed by scattering (see gray solid curve in figure 1). The time delay of the reflected wave in this case may be very different from that determined by propagation to the cut off and back as observed in the numerical computations [5]. The criteria on the density perturbation level following from condition $Z>1$, at which reflection in the BR layer appears to be substantial, takes the following form

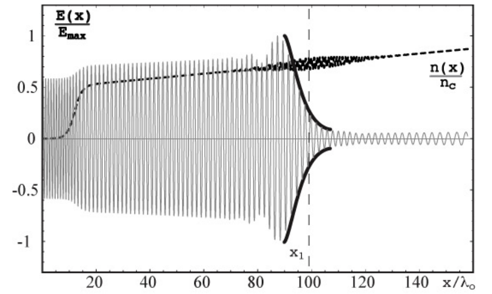

Figure 1. Normalized electric field (gray solid curve) and density (black dashed curve) distributions in sub-critical case for single perturbation centered at the Bragg resonance position. Black solid line is envelope of the normalized electric field given by analysis based on (2). Density gradient length is $390\lambda_0$, δ=7.5%

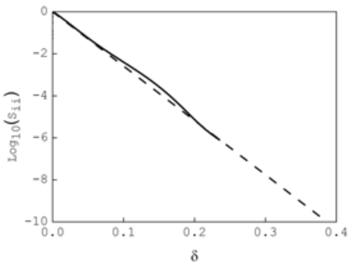

Figure 2. Dependence of transmission on the relative perturbation amplitude. Analytical formula (4) (dashed curve), simulation (solid curve). (The density gradient length is equal to $52\lambda_0$.)

$$\left.\frac{\delta n}{n}\right|_{x=x_{BR}}\geq\frac{\delta n_{th}}{n}=\left.\frac{c^2}{\omega^2}\frac{\kappa}{h_\alpha l}\frac{n_c}{n}\right|_{x=x_{BR}} \tag{4}$$

The strong BBS reflection criteria in large fusion devices may be satisfied at rather low level of density perturbation. For instance, in the case of O-mode probing from the low magnetic field side in ITER (scenario with the modestly flat density profile, $n_0=1.2\cdot10^{20}m^{-3}$, $n_{edge}=0.8\cdot10^{20}m^{-3}$, $B_0=5\ T$) at frequencies $f=85,90$ GHz the value of threshold appears to be in the range 0.5% – 1%, as presented in figure 3a. For the X-mode probing both from low and high magnetic field side it is higher (between 1% and 3%, as it is shown in figure 3b for frequencies $f=40,45$ GHz and $f=180,190$ GHz). In the case of absolutely flat density profile ($n_0=1.0\cdot10^{20}m^{-3}$, $n_{edge}=1.0\cdot10^{20}m^{-3}$,

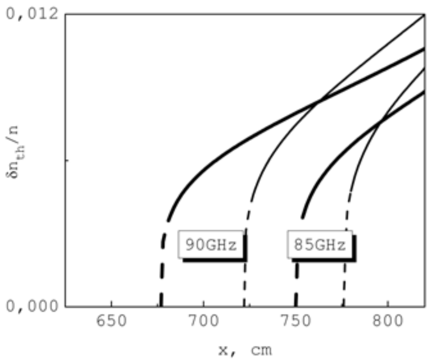

Figure 3a. Strong BBS threshold in ITER versus major radius of the BR. Solid curves correspond to the domain of the co-ordinate of BR beyond the cut-off layer, where (8) is correct. O-mode probing from the low magnetic field side for modestly flat density profile for frequencies $f = 85, 90$ GHz .

$B_0 = 5\ T$) probing of the central plasma region with O-mode is not realistic, however still possible with both low and high field side X-mode launching. As it is shown in figure 3c for uniform profile the threshold reduces substantially taking values less than 1.5% for frequencies $f = 40, 45$ GHz and $f = 170, 175$ GHz . It should be stressed that the strong BBS is the most dangerous for the X- mode high field side probing, where the probing frequency is low, so that the BBS is provided by centimeter wavelength fluctuations, for which the 1% level of relative density perturbation is usual in tokamaks. The BBS reflection effect in the later case may change strongly the time delay of the signal observed by reflectometry making density profile measurements questionable. The thermal corrections to the permittivity tensor, caused by relativistic dependencies of electron plasma and cyclotron frequencies, shown to be important for reflectometry experiment under fusion conditions and in the case of flat density profile, do not make substantial contribution to the strong BBS threshold, as it is seen in Fig. 3a in the case of O-mode reflectometry. It should be noted that the exact values of thresholds shown in figure 3 were obtained for a very simple 1D slab geometry and for specific quasi coherent density perturbations propagating in radial direction. To elucidate the main effect of strong BBS we neglected the plasma curvature effects and associated refraction and variation of poloidal wave number, as well as probing wave diffraction which affect its propagation on long trajectory substantially. As we believe, the Bragg back scattering, which is localized in narrow region near the resonance point is less sensitive to these effects and may be treated using the slab model. It is clear that the same analytical procedure leading to similar threshold condition can be applied for investigation of the quasi coherent fluctuation propagating in an arbitrary direction. However, it is as well clear that the threshold will change quantitatively for different turbulence model, nevertheless, as we are sure, the strong BBS effect as well as the main dependencies and tendencies predicted by the obtained threshold condition (4), will persist.

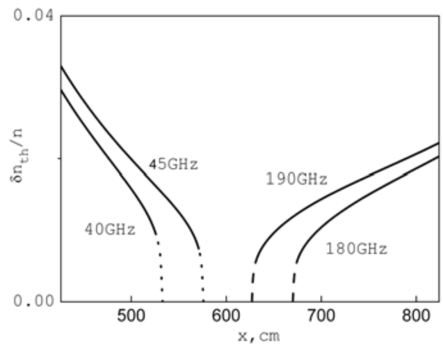

Figure 3b. Strong BBS threshold in ITER versus major radius of the BR. Solid curves correspond to the domain of the co-ordinate of BR beyond the cut-off layer, where (8) is correct. X-mode probing from high and low magnetic field side for modestly flat density profile for frequencies $f = 40, 45, 180, 190$ GHz .

4. Limitations of fluctuation reflectometry caused by the multiple small angle scattering.

Even more severe limitations to the reflectometry, as turbulence diagnostics, are put by the non linear regime of small angle scattering or, in other words, by strong phase modulation of the probing wave due to propagation in the turbulent plasma. The criterion for the reflectometry transition to the small angle scattering non linear regime is equivalent to the condition of the strong coherent wave extinction, which is reached for phase fluctuations RMS exceeding unity. According to [6, 7], in the case of linear refractive index profile and homogeneous density perturbation RMS profile the reflected wave phase fluctuation RMS for the ordinary mode probing is given by

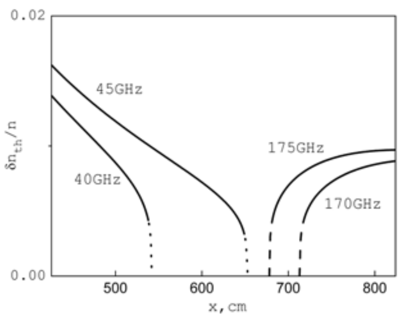

Figure 3c. Strong BBS threshold in ITER versus major radius of the BR. Solid curves correspond to the domain of the co-ordinate of BR beyond the cut-off layer, where (8) is correct. X-mode probing from high and low magnetic field side for absolutely flat density for frequencies $f = 40, 45, 170, 175$ GHz .

$$\sigma = 4\frac{\omega^2 x_c}{c^2}\cdot h_\alpha^2 \frac{\delta n^2}{n_c^2}\int_{-\infty}^{\infty}\frac{d\kappa}{2\pi}\frac{\tilde{n}_\kappa^2(0)}{|\kappa|}\left|F\left[\sqrt{\kappa x_c}\right]\right|^2 \qquad (5)$$

where

$$\left\langle \delta n(x',t')\delta n(x'',t'')\right\rangle = \delta n^2 K_n\left(x'-x'',t'-t''\right) = \delta n^2\int_{-\infty}^{\infty}\tilde{n}_\kappa^2\left(t'-t''\right)\exp\left[i\kappa\left(x'-x''\right)\right]\frac{d\kappa}{2\pi} \qquad (6)$$

and $F(s)=\int_0^s \exp\left(i\varsigma^2\right)d\varsigma$ is a Fresnel integral. Its asymptotic behavior at $s \gg 1$ is given by $F(s)\approx\sqrt{\pi}/2\cdot\exp(i\pi/4)$ whereas at $s \ll 1$ this integral is estimated as $F(s)\approx s$ .It should be emphasized, that poor localized small angle scattering, which in 1D model is produced by small wave numbers, makes substantial contribution to this integral because of $|\kappa|^{-1}$ singularity, so that for large plasma, where the distance from the edge to cut off is much larger than the turbulence correlation length ($x_c \gg l_c$), its value can be estimated with logarithmic accuracy as

$$\sigma \propto \omega^2/c^2\cdot h_\alpha^2\delta n^2/n_c^2\cdot l_c x_c \ln\left(x_c/l_c\right) \qquad (7)$$

In the case of Gaussian spectrum

$$\tilde{n}_\kappa^2(0)=\sqrt{\pi}l_c\exp\left(-l_c^2\kappa^2/4\right) \qquad (8)$$

a more accurate evaluation results in the following expression:

$$\sigma \simeq \sqrt{\pi}\frac{\omega^2 l_c x_c}{c^2}\cdot h_\alpha^2\frac{\delta n^2}{n_c^2}\left[\ln\left(\frac{8x_c}{\pi l_c}\right)+0.71\right] \qquad (9)$$

In the case of arbitrary density and/or turbulence RMS profiles expression (7) and (9) calculated in the cut off will still provide a rough estimation of the phase RMS, after substituting the local squared refractive index gradient scale length instead of x_c. Even better estimation of the phase RMS, according to [10] may be obtained in the case of Gaussian spectrum using the integral formula derived in [6]. As it was shown in [6] transition to the non-linear regime where the probing line is no longer observable in the reflected spectrum occurs when the criterion $\sigma \ge 1$ is fulfilled. Assuming homogeneous density perturbation RMS profile, we can represent the threshold of the turbulence level corresponding to the transition of the small angle scattering into the nonlinear regime as

$$\frac{\delta n}{n} > \frac{\delta n_{th}}{n}\bigg|_{c} = \frac{n_c}{h_\alpha n}\frac{c}{\omega}\frac{1}{\sqrt{l_c x_c}}\left[\ln\left(\frac{8x_c}{\pi l_c}\right)+0.71\right]^{-1/2} \tag{10}$$

The spectrum of the reflected wave (multiple scattering spectrum) in this nonlinear regime is given by expression

$$p_s(\omega-\Omega) \simeq \exp\left\{-2\left[\omega-\Omega\right]^2/\Omega_r^2\right\}, \tag{11}$$

$$\Omega_r^2 = \frac{2x_c}{\pi}\frac{\omega^2}{c^2}h_\alpha^2\frac{\delta n^2}{n_c^2}\int\frac{d\kappa}{|\kappa|}\frac{\partial^2\left[\tilde{n}_\kappa^2(\tau)\right]}{\partial\tau^2}\bigg|_{\tau=0}\left|F\left[\sqrt{\kappa x_c}\right]\right|^2 \tag{12}$$

It is no longer related to the spectrum of individual density fluctuations existing in plasma. It is rather averaged over them and possesses width determined by the number of scatterings. Namely, the spectrum width is proportional to the typical fluctuation frequency, but enhanced by the phase RMS. The later, in its turn, is proportional to the turbulent density fluctuation RMS and to the ratio of the density gradient scale and turbulence correlation length which is very large in the reactor scale device. For the modestly flat ITER density profile the threshold is estimated from (10) as $\delta n/n_c \sim 0.1 \div 1\%$ for O-mode reflectometry and $\delta n/n_{\text{X mode cut-off}} \sim 0.05 \div 1\%$ (see figure 4 where the threshold (10) is shown against the position of the cut-off for the radial correlation length corresponding to the largest value of the growth rate of the ITG mode $k_\perp\rho_i \sim 0.3$, $k_\perp = 2l_c^{-1}$, ρ_i is the deuterium gyro radius)

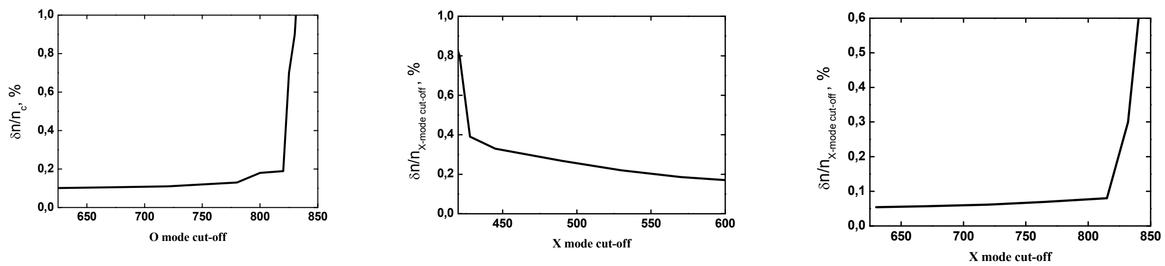

Figure 4 Threshold of the turbulence level corresponding to the transition of the small angle scattering into the nonlinear regime versus the position of the cut-off. (a) ordinary wave; (b) extraordinary wave launched from the high magnetic field side; (c) extraordinary wave launched from the low magnetic field side.

5. New approach to turbulence diagnostics based on radial correlation reflectometry

As it was shown in the previous section the application of the standard fluctuation reflectometry in reactor scale machine is questionable. Nevertheless a different approach to the turbulence diagnostics utilizing reflectometry is possible there. This alternative approach is based on the theoretical analysis of radial correlation reflectometry in strongly non-linear regime performed in [6] and [7]. As it was shown in [6,7], under condition

$$\frac{\omega^2 l_c x_c}{c^2} \cdot h_\alpha^2 \frac{\delta n^2}{n_c^2} >> 1 \tag{13}$$

when the small angle scattering is already deep in the non-linear regime, the following simple expression for the radial correlation reflectometry CCF for signals at slightly different probing frequencies is valid:

$$CCF = \exp\left(-\kappa_r^2 \Delta^2 / 2\right), \tag{14}$$

where $\Delta = x_c\left(\omega_1\right) - x_c\left(\omega_2\right)$ and

$$\kappa_r^2 = \frac{\omega^2 x_c}{2c^2} \frac{\delta n^2}{n_c^2} h_\alpha^2\Big|_c \int |\kappa| \tilde{n}_\kappa^2(0)\, d\kappa \tag{15}$$

The effective radial correlation length of the radial correlation reflectometry obtained from (15) for the Gaussian wave number spectrum is given by $\kappa_r^{-1} = l_{cx}^{ef} \simeq \left(l_{cx} / \sqrt{\pi} x_c\right)^{1/2} c/\omega\left[\delta n(x_c)/n_c\right]^{-1}$. This prediction was confirmed by comparison with results of 1 D and 2 D numerical modelling [8, 9]. It is important to note, that the signal effective correlation length here does not coincide with the turbulence radial correlation length. It is rather proportional to the square root of the turbulence correlation length and inverse proportional to the density perturbation level. As it was shown in [6, 7, 9] the information on the turbulence level provided by the effective RCR correlation length is very local. The physical reason for high locality of measurements is given by huge phase perturbation of the first probing wave gained in the region evanescent for the second.

6. Conclusions

The most sever limitations to the reflectometry application in reactor scale fusion devices are caused by strong phase modulation of the probing wave on the long trajectory. The threshold of this effect is overcome at the relative density perturbation level of 0.05 – 1.5 % making standard approach to the plasma micro turbulence study with fluctuation reflectometry questionable. To cope with this problem we introduce the new approach to the fluctuation reflectometry utilizing strong non-linear regime of the small angle scattering expected in the ITER and permitting localized measurements of turbulence parameters using radial correlation reflectometry. In this non-linear regime the cut off separation at which the coherence of two reflectometry signals is suppressed provide us with information not on the turbulence correlation length but on the ratio of its square root and the density perturbation amplitude.

As a result of analytical treatment performed in a simple 1D reflectometry model for quasi coherent fluctuations we may conclude that threshold conditions for strong Bragg backscattering will be met at a 1% relative density perturbation level in reactor scale magnetic fusion devices possessing flat plasma density profile. The strong BBS effect is the most dangerous for the high magnetic field side X-mode reflectometry utilizing low frequency microwaves for probing. At high turbulence level it can change substantially the time delay of the signal observed by reflectometry, which introduces big perturbations to the density profile reconstruction. It should be noted that the exact values of thresholds shown in figure 3 were obtained for specific quasi coherent density perturbations propagating in radial direction. Meanwhile, the main tendencies predicted by the obtained threshold condition (5), as we believe, will persist. Nevertheless, because of important role the BBS may play in reflectometry experiment in large fusion devices, a further development of nonlinear BBS theory, accounting for a more realistic turbulence spectra and experimental geometry is highly desirable.

7. Acknowledgements

Financial support by RFBR (grants 09-02-00453, 07-02-92162-CNRS), NWO-RFBR Centre of Excellence on Fusion Physics and Technology (grant 047.018.002), ANR_blanc_06_0084, scientific school grant-1550.2008.2 and by Dynasty Foundation is acknowledged.

8. References

[1] G. Vayakis, C.I. Walker, F. Clairet et al 2006 *Nucl. Fusion* **46** S836-S845

[2] A R Polevoi, M Shimiada *et al* 2005 *Nucl. Fusion* **45** 1451

[3] G.J. Kramer, R. Nazikian, E.J. Valeo et al 2006 *Nucl. Fusion* **46** S846–S852

[4] E.Z. Gusakov, S. Heuraux, A.Popov 2009 *Plasma Phys. Control. Fusion* **51** 065018

[5] S Hacquin, S Heuraux, M Colin, G Leclert 2001 *Journal of Computational Phys.* **174** 1

[6] E Z Gusakov and A Yu Popov 2002 *Plasma Phys. Control. Fusion* **44** 2327;

[7] E Z Gusakov and A Yu Popov 2004 *Plasma Phys. Control. Fusion* **46** 1393–1408

[8] Valeo E J, Kramer G Y and Nazikian R 2002 *Plasma Phys. Control. Fusion* **44** L1; Kramer G Y, Valeo E J and Nazikian R 2003 *Rev. Sci. Instrum.* **74** 1421

[9] G Leclert, S Heuraux, E Z Gusakov et al. 2006 Plasma Phys. Control. Fusion 48 1389–1400

[10] M Shubert, F Clairet, F da Silva et al. In IRW9 proceedings http://www.ipfn.ist.utl.pt/irw9/papers/mschubert_paper.pdf